Investigation of single proton dissociation

Nataliia Chudak (Odesa Polytechnic), Oleksii Potiienko (Odesa Polytechnic),
Denys Zhuravel (BITP, Kyiv)

This project has received funding through the EURIZON project, which is funded by the European Union under grant agreement No.871072

Romania, 2024

Schematic of the diffraction scattering of hadrons

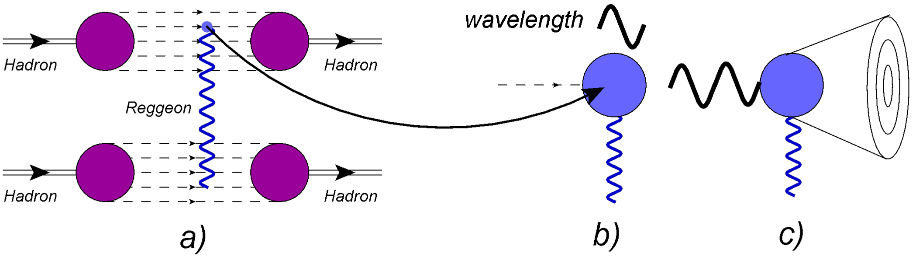

Figure 1: (a) Reggeon exchange between the structural components of hadrons. (b) Relationship between the wavelength of the structural component and the size of the interaction region. (c) Diffraction of the structural component on the interaction region

Optical analogy for diffraction particle production

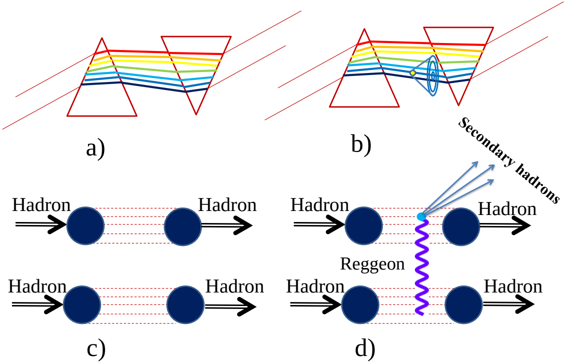

Figure 2: (a) Decomposition and recombination of white light: passing through two prisms. (b) Diffraction effects of a particle between two prisms: formation of secondary beams alongside the white beam. (c) Decomposition of hadronic states into component states: analogy with white light and prisms. (d) Effect of Reggeon scattering on hadronic states: formation of secondary particles.

$$p + p \to p + X,$$

where p is proton, X is a system of secondary hadrons.

$$\frac{d^2\sigma}{dtdM_x^2} \approx \frac{9\beta^4}{4\pi}\left[F^p(t)\right]^2\left(\frac{s}{M_X^2}\right)^{2(\alpha_P(t)-1)}\frac{W_2\left(t, M_x^2\right)}{2m}$$

where

- t is the momentum transfer between colliding particles
- s is the square of the center-of-mass energy of the collision
- β is the quark-Pomeron coupling
- m is proton mass
- $W_2(t, M_x)$ is a structure function of proton
- $\alpha_P(t) = 1.08 + 0.25t$ is the Pomeron trajectory
- $F^p(t) = (1.0 - t/0.71)^{-2}$ is the proton elastic form factor

$$\mathbf{W_2(t, M_x)} \to \textbf{ deep inelastic scattering (DIS)}$$

L. L. Jenkovszky, O. E. Kuprash, J. W. Lamsa, V. K. Magas, and R. Orava. Dual-regge approach to high-energy, low-mass diffraction dissociation. Phys. Rev. D, 83:056014, Mar 2011

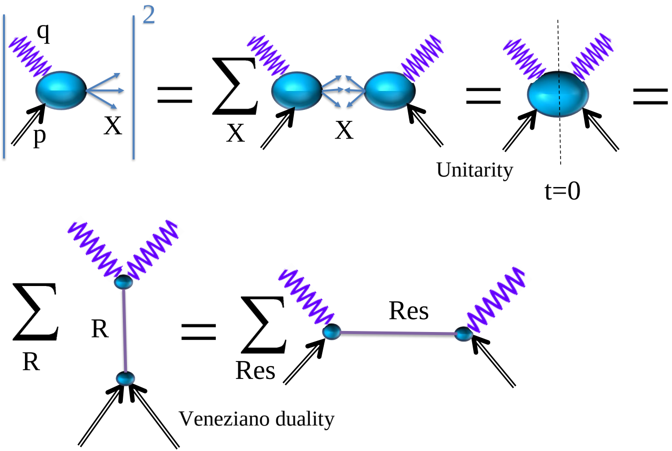

Figure 3: Connection, through unitarity and Veneziano-duality, between the inelastic form factor and the sum of direct-channel resonances.

$$\frac{d^2\sigma}{dtdM_x^2}\left(M_x^2,t\right)=A_0\left(\frac{s}{M_x^2}\right)^{2\alpha_p(t)-2}\frac{x(1-x)^2[F^p\left(t\right)]^2}{\left(M_x^2-m^2\right)\left(1-4m^2x^2/t\right)^{3/2}}$$
$$\times\sum_{n=1}^{3}[f\left(t\right)]^{2(n+1)}\frac{\operatorname{Im}\alpha\left(M_x^2\right)}{[2n+0.5-\operatorname{Re}\alpha\left(M_x^2\right)]^2+[\operatorname{Im}\alpha\left(M_x^2\right)]^2}$$

where

- $A_0 = 9a\beta^4/\pi\alpha_{fs}$ is the normalization factor
- α_{fs} is fine structure constant
- $x = -t/2m\nu$ is Bjorken variable
- $\nu = \left(M_X^2 - m^2 - t\right)/2m$ is kinematic variable
- $f(t) = (1 - t/t_0)^{-2}$ is the form factor of $\mathbb{P}p \to \mathbb{P}p$ system
- t_0 is the model parameter
- $\alpha\left(M_X^2\right)$ is the (nonlinear complex) baryonic resonance trajectory in M_X^2 channel, which allows to account for a set of various resonances

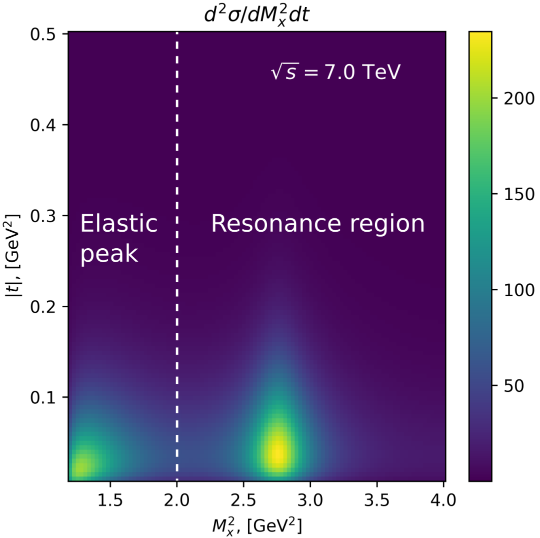

Figure 4: The differential cross-section $d^2\sigma/dtdM_X^2$ in t, M_X^2 plane. There are two missing mass M_X regions: elastic peak region ($M_X^2 < 2$ GeV^2), and the resonance region (2 GeV$^2 \leqslant M_X^2 \leqslant 8$ GeV^2).

The behavior of the differential cross-section in the $(t,\ M_X^2)$ plane

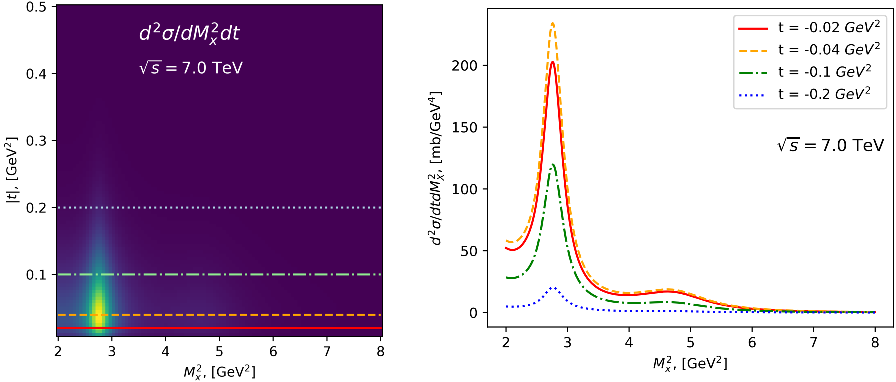

Figure 5: The differential cross-section $d^2\sigma/dtdM_X^2$ in the t, M_X^2 plane in the resonance region for $0 \leqslant -t \leqslant 0.5$ GeV^2 (left), and multiple regular plots in M_X^2 at fixed values of t (right).

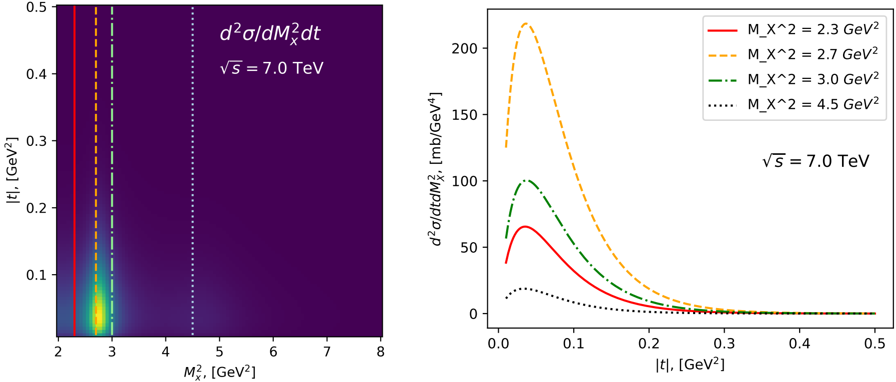

Figure 6: The differential cross-section $d^2\sigma/dtdM_X^2$ in the t, M_X^2 plane in the resonance region for $0 \leqslant -t \leqslant 0.5$ GeV^2 (left), and multiple regular plots in t at fixed values of M_X^2 (right).

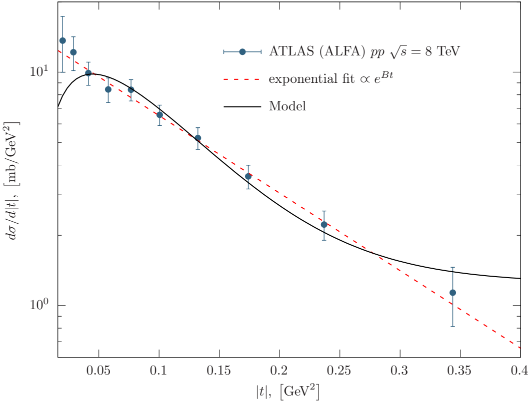

Figure 7: The differential cross-section $d\sigma/dt$ of single diffraction dissociation as a function of $|t|$. The dashed line is the exponential fit to the experimental data. The solid line is the model fit with the constant background contribution b_0.

The fitting procedure converges with $\chi^2/d.o.f. \approx 1.07$, providing the following values of parameters: $A_0 = 35.58$ mb/GeV^2, $t_0 = 1.486$ GeV^2, and $b_0 = 8.2$ mb/GeV^2.

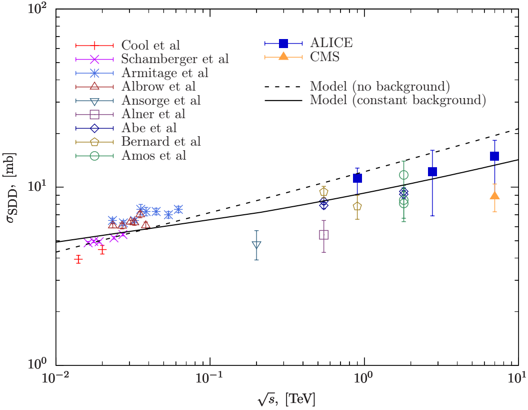

Figure 8: The total single diffraction dissociation cross-section as a function of $\sqrt{s}$. The dashed line is the model fit to the experimental data without any background contribution. The solid line is the fit with the constant background contribution b.

The values of parameters in this case are $A_0 = 378.43 \pm 16.68$ mb/GeV^2 and $b = 1.85 \pm 0.16$ mb/GeV^2.

Summary

- The in-depth examination of the differential cross-sections behavior within the resonance region is performed, particularly at low missing masses M_X
- The fits of $d\sigma_{SDD}/dt$ and σ_{SDD} were performed using C++ programs within the ROOT framework, specifically employing Minuit for parameter optimization
- Results are presented as numerical values of parameters, goodness-of-fit metrics, and graphical representations

Thank you for your attention!